Wave Electronics, 3 (1977) 35—49

SURFACE-ACOUSTIC-WAVE PROPERTIES IN ZnO-SiO_2-Si LAYERED STRUCTURE

SHUSUKE ONO, KIYOTAKA WASA and SHIGERU HAYAKAWA

Materials Research Laboratory, Matsushita Electric Industrial Co., Ltd, Kadoma, Osaka 571 (Japan)

(Received August 27, 1976; in revised form October 8, 1976)

Summary

Calculations have been made for a surface-acoustic-wave phase velocity, group velocity, their temperature coefficients and an effective electromechanical coupling factor in a layered structure ZnO-SiO_2-Si. It is found that , in the layered structure, the temperature coefficient of the phase velocity ranges nearly from —30 to +80 ppm/° C, while one of the group velocity from —50 to +130 ppm/° C. The highest coupling is achieved by the layered structure which is constructed on the (001) cut <100> and <110> propagating Si substrate for the first peak of the coupling factor and the (011) cut <110> propagating Si substrate for the second peak, when the ZnO layer has the *c*-axis normal to the substrate surface.

1. Introduction

With the increasing use of surface-acoustic-wave (SAW) devices in various applications, the need for materials with high electromechanical coupling and temperature stability is becoming increasingly more important. A ST-cut quartz is the best-known temperature-stable material, but its usefulness is limited because of its very low coupling. On the other hand, $LiNbO_3$ is the well-known material with high coupling, but its stability is very poor. New temperature-stable materials with high coupling have been sought, but have not yet been produced [1]. In another approach, combined materials, i.e. film overlays on appropriate substrates, have been studied. Piezoelectric ZnO on nonpiezoelectric fused quartz has higher coupling than the semi-infinite ZnO [2, 3]. Although nonpiezoelectric SiO_2 on YZ-$LiNbO_3$ and YZ-$LiTaO_3$ has high coupling and a zero-temperature coefficient of a delay time [4], it is not compatible for integrated circuit devices to which SAW devices will normally be connected. The SAW devices with the Si substrate have been investigated theoretically or experimentally; Al_2O_3-ZnO-Si and ZnO-Al_2O_3-Si three-layer structures relating to a nearly dispersion-free propagation [5], CdS-SiO_2-Si to a high electromechanical coupling [6], ZnO-SiO_2-Si to a SAW convolver [7, 8], etc.

Among various piezoelectric films commonly used, highly-oriented ZnO

films with the c-axis normal to the substrate have the highest coupling. Fabrication techniques for these are well-established at present [3, 9]. Since a temperature coefficient of the SAW velocity TC(v), defined by $(1/v)\,(dv/dT)$ (hereafter, a similar notation is used for other properties), is positive for both ZnO and Si, one more material with a negative TC(v) should be combined in order to obtain the temperature-compensated structure comprising ZnO and Si. SiO_2 is a well-known material having such a property and is suitable for the integrated circuit devices.

For some SAW devices, zero-temperature coefficient of center frequency of interdigital transducers, determined by the temperature coefficient of the phase velocity TC(v_p), is desired. Zero-temperature coefficient of delay time, which should be determined by one of the group velocities TC(v_g) in dispersive media such as a layered structure, is also very important for some SAW devices.

This paper describes the SAW properties in the layered structure ZnO-SiO_2-Si, in which the piezoelectric ZnO layer has the c-axis normal to the surface. The phase velocity v_p, the group velocity v_g, their temperature coefficients TC(v_p), TC(v_g) and the coupling factor $\Delta v/v$ are calculated by using a computer. The thickness of the ZnO and SiO_2 layers and crystallographic orientations of the Si substrate are discussed, for which the ZnO-SiO_2-Si structure yields high electromechanical coupling and temperature-stability. Various effects on TC(v_p) and TC(v_g), caused by the difference of thermal expansion coefficients in the layer and the substrate, are also discussed.

2. Method and results of calculations

For the purpose of determining a SAW phase velocity v_p in a layered structure ZnO-SiO_2-Si, a matrix formulation has been used, which is essentially similar to that of Ingebrigsten—Tonning [10]and is extended to include piezoelectric effects. A group velocity v_g of the SAW, propagating with wave vector k, has been calculated by using v_p; $v_g = \partial(kv_p)/\partial k$. A computer program has been written to perform numerical calculations of v_p and $\partial v_p/\partial k$. A cross section of the structure and coordinate axes are shown in Fig.1. The following specifications and assumptions are made to examine the characteristic features of SAW propagating on the layered structure.

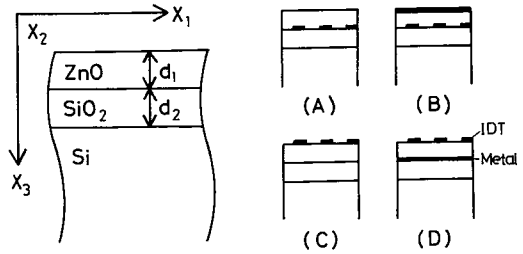

Fig.1. Cross section of the layered structure ZnO-SiO_2-Si. Interdigital transducers (IDT) and shorting metals are shown in four different configurations (A), (B), (C) and (D).

(1) The ZnO layer with a thickness d_1 is a single crystal (6mm) and its c-axis normal to the substrate surface.

(2) The SiO_2 layer with a thickness d_2 is electrically and elastically equivalent to fused quartz.

(3) The substrate with a half-space is (001), (011) and (111) cut single crystal Si or polycrystalline Si.

The surface and interface are coplanar with the x_1-x_2 plane. The SAW with wave vector k propagates along the x_1-axis and is a straight-crested wave, in which components of mechanical displacements and electric potential are invariant in the x_2-direction.

Since both the c-cut ZnO and SiO_2 layers can be considered as isotropic media for the SAW propagation, crystallographic orientations of the ZnO-SiO_2-Si structure are characterized only by those of the Si substrate. When the SAW propagates along the $<11\bar{2}>$ axis of the (111) cut single crystal Si, for example, the layered structure may be named as ZnO-SiO_2-$Si_{(111)<11\bar{2}>}$. On the poly-crystalline Si, named as ZnO-SiO_2-$Si_{(poly)}$.

Material constants used in this paper are listed in Table 1. Temperature co-

TABLE 1

Material constants at room temperature; density ρ (g/cm^3), elastic C^E (10^{11} N/m^2), piezoelectric e (C/m^2), dielectric ϵ^S ($\times \epsilon_0$), thermal expansion coefficient β (ppm/° C) and temperature coefficient of elastic constants TC(C^E) (ppm/° C)

Material	ZnO	SiO_2	crystal-Si	poly-Si
ρ	5.676	2.2	2.331	2.331
$C_{11}{}^E$	2.096	0.785	1.657	1.865
$C_{33}{}^E$	2.109			
$C_{12}{}^E$	1.211	0.161	0.639	0.535
$C_{13}{}^E$	1.051			
$C_{44}{}^E$	0.425	0.312	0.796	0.665
e_{31}	−0.61			
e_{33}	1.14			
e_{15}	−0.59			
$\epsilon_{11}{}^S$	8.33	3.8	11.8	11.8
$\epsilon_{33}{}^S$	8.84			
β_1	4.0	0.55	2.6	2.6
β_3	2.1			
TC($C_{11}{}^E$)	−112	239	−68	−65
TC($C_{33}{}^E$)	−123			
TC($C_{12}{}^E$)	−144	584	−100	−112
TC($C_{13}{}^E$)	−161			
TC($C_{44}{}^E$)	− 70	151	−44	−46
Reference	[11, 13, 16, 17]	[12, 14]	[11, 14, 15]	[11]

efficients of elastic constants TC(C^E) for the ZnO crystal were estimated by using measured values of TC(S_{11}^E), TC(S_{12}^E), TC(S_{55}^E) and TC(C_{33}^D) [17] on the assumption that TC(S_{13}^E) = TC(S_{12}^E) and TC(C_{33}^E) = TC(C_{33}^D). Thermal expansion coefficients β_1 and β_3 of ZnO have not been measured; for estimation it was assumed that they were the same as those of a hexagonal (wurtzite) CdS which has similar lattice properties to the ZnO crystal. Elastic constants of the polycrystalline Si were estimated from those of the single crystal Si by using a Hill approximation [11].

The results of numerical calculations are described as follows.

2.1 Velocity

Typical thickness dependences of v_p and v_g are shown in Figs.2 and 3, respectively. In these figures, the ZnO-SiO_2 structure is described by $kd_2 = \infty$ (curve 4). It has been found that the SAW for ZnO-SiO_2-$Si_{(111)<1\bar{1}2>}$, -$Si_{(001)<100>}$, -$Si_{(001)<110>}$, -$Si_{(011)<100>}$, -$Si_{(011)<01\bar{1}>}$ and -$Si_{(poly)}$ is a Rayleigh-type wave which is polarized in a sagital plane (x_1—x_3 plane).

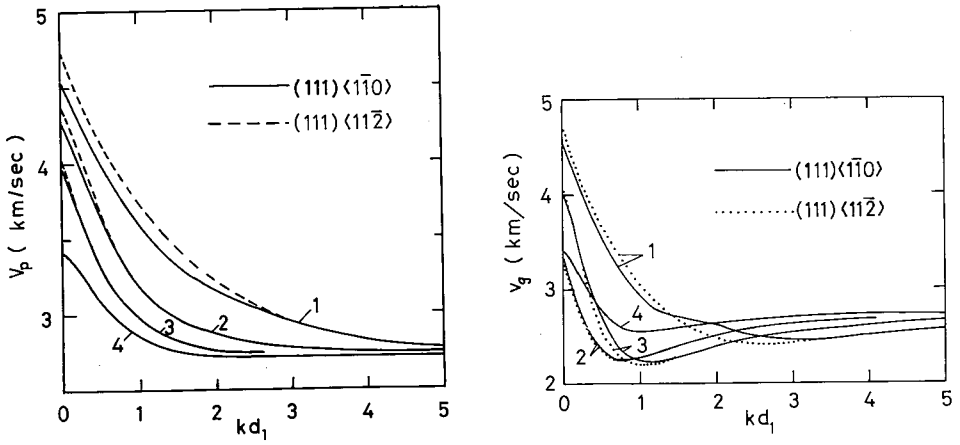

Fig. 2. Phase velocity v_p as a function of the ZnO layer thickness kd_1 for ZnO-SiO_2-$Si_{(111)<1\bar{1}0>}$ and -$Si_{(111)<11\bar{2}>}$. The SiO_2 layer thickness kd_2 is 0.0 (curve 1), 1.0 (2), 2.0 (3) and ∞ (4).

Fig. 3. Group velocity v_g as a function of the ZnO layer thickness kd_1 for ZnO-SiO_2-$Si_{(111)<1\bar{1}0>}$ and -$Si_{(111)<11\bar{2}>}$. The SiO_2 layer thickness kd_2 is 0.0 (curve 1), 1.0 (2), 2.0 (3) and ∞ (4).

That is, it does not possess a component of mechanical displacements u_2 in the x_2-direction, while the SAW for ZnO-SiO_2-$Si_{(111)<1\bar{1}0>}$ is a complicated wave with non-zero u_2. For these layered structures, v_p and v_g are equal in direction, but different in magnitude as shown in Fig.4, which expresses the difference of two velocities $(v_p - v_g)/v_p$ due to dispersion. The SAW, propagating along the poor symmetry axis on the (001), (011) and (111) cut Si substrate, gives thickness dependences of v_p and v_g qualitatively similar to those shown in

Figs.2 and 3, although they possess non-zero angle θ between directions of v_p and v_g. Figure 5 describes typical magnitudes of θ, which also means the direction of energy flow measured from that of the phase propagation (x_1-axis).

The maximum value of v_p and v_g, which occurs at $kd_1 = kd_2 = 0$ (the Si substrate only), is given by Farnell [18], except that of the polycrystalline Si (4.89 km/s). For ZnO-SiO_2-$Si_{(001)<hk0>}$, in which an angle between the $<hk0>$ and $<100>$ axis ranges from about 30° to about 45°, the SAW approaches the pseudo-wave or leaky-wave given by Farnell [18]as both kd_1 and kd_2 decrease.

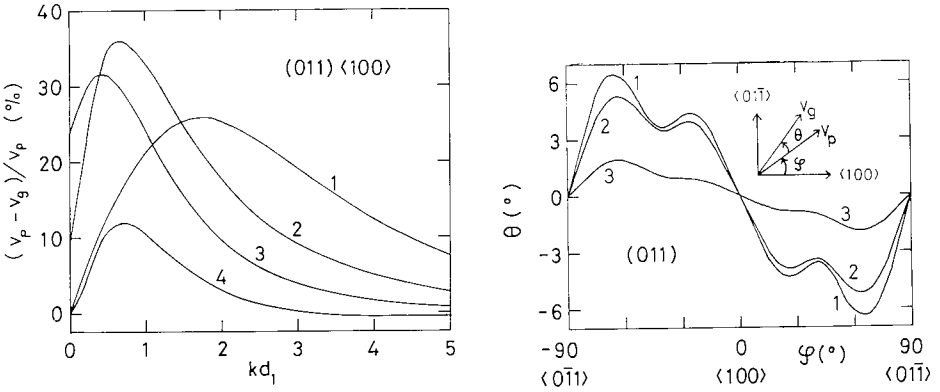

Fig.4. Difference of the phase and group velocities $(v_p - v_g)/v_p$ for ZnO-SiO_2-$Si_{(011)<100>}$. The SiO_2 layer thickness kd_2 is 0.0 (curve 1), 1.0 (2), 2.0 (3) and ∞ (4).

Fig. 5. Angle θ between the phase and group velocities for ZnO-SiO_2-Si with the (011) cut Si substrate. The ZnO layer thickness kd_1 is 0.2. The SiO_2 thickness kd_2 is 0.0 (curve 1), 0.6 (2) and 2.0 (3).

2.2. Temperature coefficient of velocity

An important parameter of SAW devices is the temperature coefficient of the SAW phase velocity $TC(v_p)$ and the group velocity $TC(v_g)$, by which temperature coefficients of delay time $TC(\tau)$ and center frequency $TC(f_0)$ are determined; $TC(\tau) = \beta - TC(v_g)$ and $TC(f_0) = TC(v_p) - \beta$, where β is a thermal expansion coefficient of a substrate material.

In order to investigate entire features of these temperature coefficients $TC(v_p)$ and $TC(v_g)$, they were estimated by calculating approximate ones $TC_a(v_p)$ and $TC_a(v_g)$; $TC_a(v) = (v_{RT+100} - v_{RT})/v_{RT} \times 10^4$ (ppm/° C), where v_{RT} and v_{RT+100} are velocities at room temperature (20° C) and 120° C, respectively. Thickness dependences of $TC_a(v_p)$ and $TC_a(v_g)$ are shown in Figs.6 and 7, respectively. The material constants listed in Table 1 result that both of them are −30 ppm/° C for ZnO, +85 for SiO_2 and −21 for Si which is almost independent of their crystallographic orientations. Considering the various propagation directions on the (001), (011) and (111) cut crystal and polycrystalline Si substrate, it has been found that at each thickness kd_1 and kd_2 the

largest and smallest values of TC_a (v_p) are almost given by ZnO-SiO_2-$Si_{(011)<100>}$ and - $Si_{(111)<1\bar{1}0>}$ shown in Fig.6, respectively, although ZnO-SiO_2-$Si_{(011)<01\bar{1}>}$ yields smaller values than ZnO-SiO_2-$Si_{(111)<1\bar{1}0>}$ by about 2 ppm/°C at some ranges of kd_1 and kd_2; $kd_1 \lesssim 0.5$ and $0.3 \lesssim kd_2 \lesssim 2.0$. It has also been seen that TC_a (v_g) is almost limited by ZnO-SiO_2-$Si_{(011)<100>}$ and —$Si_{(111)<1\bar{1}0>}$ shown in Fig.7 with the exception of the same order as one of $TC_a(v_p)$. Therefore, the layered structure ZnO-SiO_2-Si, having the zero-temperature coefficients of v_p and v_g is realized by using the appropriate thickness independently of the properties of the Si substrate; $kd_1 \lesssim 2.9$ and $kd_2 \gtrsim 0.3$ for v_p; $kd_1 \lesssim 2.0$ and $kd_2 \gtrsim 0.1$ for v_g.

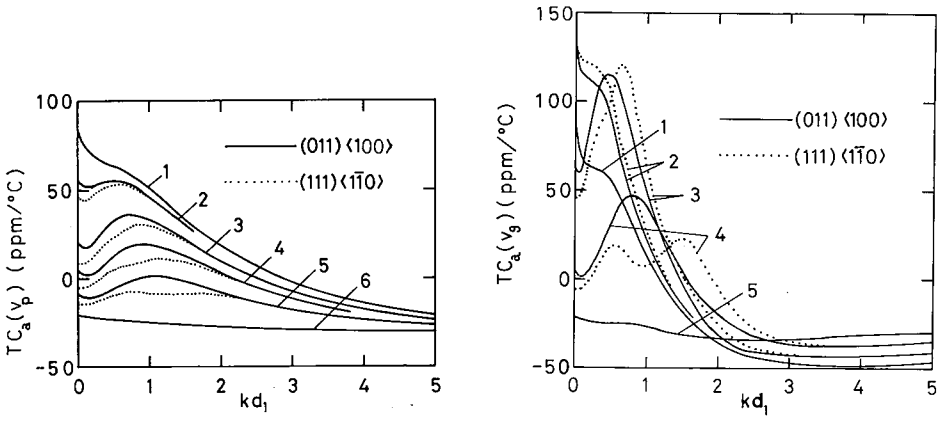

Fig.6. Temperature coefficient of the phase velocity $TC_a(v_p)$ as a function of the ZnO layer thickness kd_1 for ZnO-SiO_2- $Si_{(011)<100>}$ and -$Si_{(111)<1\bar{1}0>}$. The SiO_2 layer thickness kd_2 is ∞ (curve 1), 2.0 (2), 1.0 (3), 0.6 (4), 0.3 (5) and 0.0 (6).

Fig.7. Temperature coefficient of the group velocity $TC_a(v_g)$ as a function of the ZnO layer thickness kd_1 for ZnO-SiO_2-$Si_{(011)<100>}$ and -$Si_{(111)<1\bar{1}0>}$. The SiO_2 layer thickness kd_2 is ∞ (curve 1), 2.0 (2), 1.0 (3), 0.3 (4) and 0.0 (5).

2.3 Coupling factor Δ v/v

Another important parameter for SAW devices is a piezoelectric coupling coefficient K that is a measure of electrical to acoustical energy conversion and vice versa. K has been calculated from the relative change $\Delta v/v$ in the phase velocity v_p, when an electrically perfect conducting and elastically negligible metal film is placed at the position of the interdigital transducer (IDT) shown in Fig.1; $\Delta v/v \cong K^2/2$ approximately [19]. The typical results of the coupling factor $\Delta v/v$ are shown in Fig.8, where the layered structure is ZnO-SiO_2-$Si_{(011)<100>}$ with $kd_2 = 0.5$ and an electrical conductivity σ of the Si substrate is infinite or zero. It is obvious from Fig.8 that $\Delta v/v$ has a double-peaked character, which is well-known for ZnO-fused quartz, ZnO-$Si_{(001)<100>}$ [2]and CdS-SiO_2-$Si_{(111)<11\bar{2}>}$ [6]; the first peak at $kd_1 \simeq 0.2$ for the configurations (B) and (D) shown in Fig.1 and the second peak at $kd_1 \simeq 2.8$ for (A) and (B).

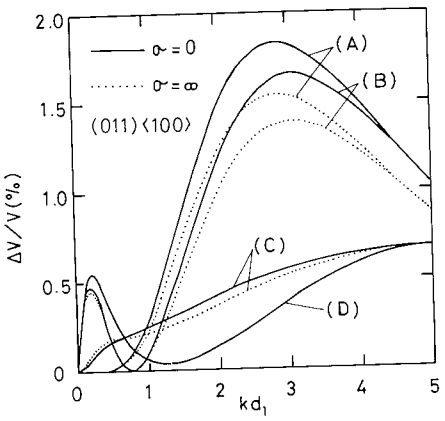

Fig.8. Coupling factor $\Delta v/v$ for the configuration (A) — (D) and the structure ZnO-SiO_2-Si $(011)\langle 100\rangle$ with $kd_2 = 0.5$. The electrical conductivity σ of the Si substrate is zero and infinite.

First peak

The layered structure in the configuration (D) has always a larger value of $\Delta v/v$ than that in (B), independently of the thickness of the ZnO and SiO_2 layers and crystallographic orientations of the Si substrate. Figure 9 indicates a directional dependence of $\Delta v/v$ in (D), where $\Delta v/v$ is independent of σ of the Si substrate. It is seen that the largest value of $\Delta v/v$ is gained by setting the propagation direction in the $\langle 100\rangle$ or $\langle 110\rangle$ axis on the (001) cut Si substrate, similarly $\langle 100\rangle$ on (011) and $\langle 11\bar{2}\rangle$ on (111). The layered structure on the polycrystalline Si substrate has $\Delta v/v$ larger than that on the (111) cut $\langle 11\bar{2}\rangle$ propagating Si, but smaller than that on the $(001)\langle 100\rangle$ Si. It is apparent from Fig.10, showing the thickness dependence of $\Delta v/v$ for ZnO-SiO_2-$Si_{(001)\langle 100\rangle}$ and the configuration (D), that there is an optimum thickness range, for which $\Delta v/v \gtrsim 0.5$ %; $kd_1 \cong 0.15$—0.38 and $kd_2 \cong 0.2$—0.7, and that the most optimum range ($\Delta v/v \cong 0.54\%$) is $kd_1 \cong 0.2$ and $kd_2 \cong 0.5$. For other layered structures and the configuration (B), similarly, an optimum range of kd_1 and kd_2 exists.

Second peak

The directional dependence of $\Delta v/v$ shows that the highest coupling is obtained by using the same propagation direction as one of the first peak, although its dependence is much smaller. The configuration (A) gives always larger $\Delta v/v$ than (B). Figure 11 shows the thickness dependence for ZnO-SiO_2-$Si_{(011)\langle 100\rangle}$ and the (A), in which the largest $\Delta v/v$ is given among various kinds of the Si substrates. The optimum range of thickness is $kd_1 \cong 2.3$—3.5 and $kd_2 \gtrsim 0.3$, for which $\Delta v/v \gtrsim 1.75\%$, and the most optimum one ($\Delta v/v \cong 1.87\%$) is $kd_1 \cong 2.8$ and $kd_2 \cong 1.0$.

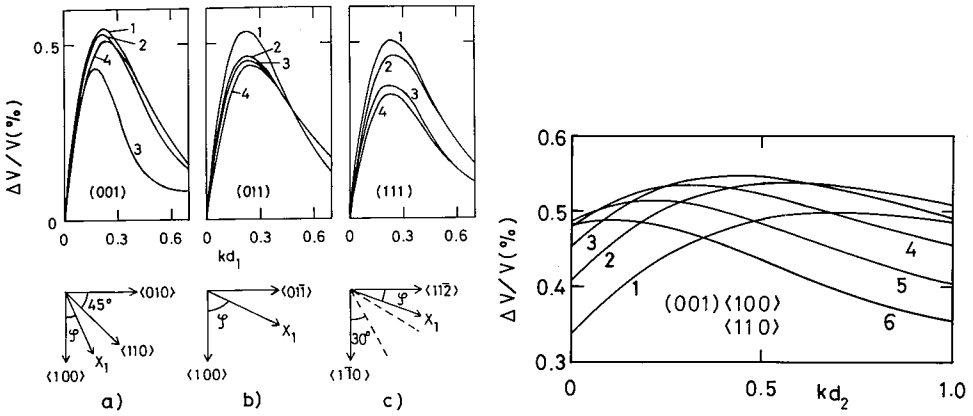

Fig.9. Coupling factor $\Delta v/v$ near the first peak for the configuration (D) and the structure ZnO-SiO_2-Si with kd_2 = 0.6. The substrate is (a) the (001)-cut Si crystal with φ = 0° (curve 1), 15° (2), 30° (3), 40° (4) and 45° (1); (b) the (011) Si with φ = 0° (1), 30° (2), 60° (3) and 90° (4); (c) the polycrystalline Si (curve 1) and the (111)-cut Si crystal with φ = 0° (2), 15° (3) and 30° (4).

Fig.10. Coupling factor $\Delta v/v$ near the first peak for the configuration (D) and the structure ZnO-SiO_2-$Si_{(001)<100>}$ or -$Si_{(001)<110>}$. The ZnO layer thickness kd_1 is 0.15 (curve 1), 0.2 (2), 0.25 (3), 0.3 (4), 0.35 (5) and 0.4 (6).

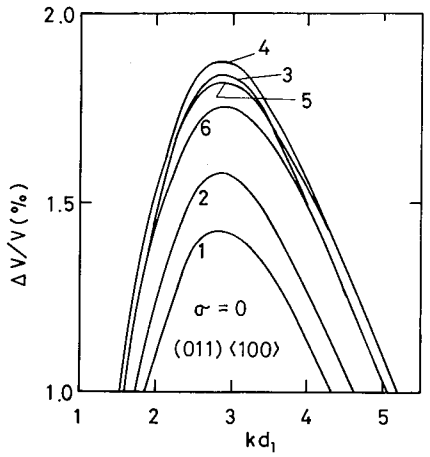

Fig.11. Coupling factor $\Delta v/v$ near the second peak for the configuration (A) and the structure ZnO-SiO_2-$Si_{(011)<100>}$. The conductivity σ of the Si substrate is zero. The SiO_2 layer thickness kd_2 is 0.0 (curve 1), 0.1 (2), 0.5 (3), 1.0 (4), 2.0 (5) and ∞ (6).

3. Discussion

3.1 Velocity

The phase velocity v_p shown in Fig.2 and the group velocity v_g in Fig.3 are ones for the SAW propagating on the ZnO-SiO_2-Si layered structure without

shorting metals at both surfaces of the ZnO layer. It is apparent from $\Delta v/v$ shown in Fig.8 that the changes of v_p and v_g due to shorting metals are, at most 1.8%.

For some devices, such as a delay line, the angle θ between directions of the energy flow and the phase propagation is an important parameter when the SAW propagates along the poor symmetry axis of the Si substrate as shown in Fig.5. The smallest value of v_g, which is also important, is given by $ZnO\text{-}SiO_2\text{-}Si_{(011)<100>}$ with $kd_1 \cong kd_2 \cong 1.0$; $v_g \cong 2.16$ km/s. For this layered structure, however, the temperature coefficient of v_g is large; $TC_a(v_g) \cong 49$ ppm/° C. The layered structure, having small v_g (2.23 km/s) and the zero-temperature coefficient of delay time, is realized by the same layered structure except that $kd_1 \cong 1.4$.

The thickness dependences of v_p and v_g, however, have only a qualitative meaning for the layered structure, in which the ZnO layer is prepared by thin film technology such as sputtering, because elastic constants of films are different from those of single crystals and an internal stress is induced during fabrication of films. For example, the SAW phase velocity in sputtered ZnO films is about 2.54 km/s [3], while in ZnO crystals it is 2.72 km/s. The variation of the phase velocity due to the internal stress σ_{11} in the direction of the SAW propagation is estimated as follows. Since equations determining the phase velocity, include σ_{11} only in the form $(\rho v_p^2 - \sigma_{11})$ [20], the variation δv_p becomes approximately

$$\delta v_p/v_p \cong \sigma_{11}/(2 \rho v_p^2), \tag{1}$$

where ρ is the density of the film. Using the fact that the magnitude of σ_{11} is 10^8—10^9 N/m^2 [21], $\delta v_p/v_p$ becomes about 10^{-3}—10^{-2}. The contribution of the internal stress is the minor factor. Therefore, the difference in v_p seems to be mainly caused by the difference between elastic constants.

3.2 Temperature coefficient of velocity

In the preceding section the approximate temperature coefficients $TC_a(v_p)$ and $TC_a(v_g)$ have been estimated on the assumption that the density ρ and elastic constants C^E vary linearly with temperature, that is, $TC(\rho)$ and $TC(C^E)$ are constant. This assumption is reasonable as long as the linear temperature coefficient $TC(v)$ (v represents v_p or v_g) is concerned. In order to obtain the exact $TC(v)$ from the approximate $TC_a(v)$, one should consider the following effects on $TC(v)$; $TC_1(v)$ due to non-linear temperature dependence of v, $TC_2(v)$ due to non-zero $TC(e)$ and $TC(\epsilon^S)$, $TC_3(v)$ due to the thermal expansion for the layer thickness, $TC_4(v)$ due to the change of $TC(\rho)$ in the layer caused by the difference of thermal expansion coefficients in the layer and the substrate, and $TC_5(v)$ due to the internal stress induced by the same origin as $TC_4(v)$.

In order to estimate the effect $TC_1(v)$, the relative temperature dependences $R(v_p)$ and $R(v_g)$ have been calculated; $R(v) = [v(\Delta T) - v_{RT}]/v_{RT}$. v_{RT} and $v(\Delta T)$ are velocities at room temperature and at the temperature measured

from it, respectively. Figure 12 shows examples of $R(v_p)$ for the ZnO-SiO_2 structure with $kd_1 \simeq 2.9$ and $kd_2 = \infty$ and for ZnO-SiO_2-$Si_{(011)<100>}$ with $kd_1 = 0.2$ and $kd_2 \simeq 0.55$, in which $TC(v_p)$ is nearly zero as shown in Fig.6. In Fig.12 an exact temperature coefficient $TC(v_p)$ is determined by the slope of $R(v_p)$ at room temperature ($\Delta T = 0°$ C), while an approximate value, $TC_a(v_p)$, is determined by the slope of the straight line connected with $R(v_p)$ at $\Delta T = 0$ and 100° C. It is found from Fig.12 that the difference between $TC(v_p)$ and $TC_a(v_p)$, i.e. the effect $TC_1(v_p)$ due to non-linearity of v_p, is about 0.2 ppm/° C for the ZnO-SiO_2 structure and 0.4 for ZnO-SiO_2-Si. It is also found from numerical calculations of $R(v_g)$ that the effect $TC_1(v_g)$ is the same order as $TC_1(v_p)$. Therefore, it is reasonable to neglect the effect $TC_1(v)$, although the nonlinear behaviour of the velocities is remarkable for the layered structure having small temperature coefficients.

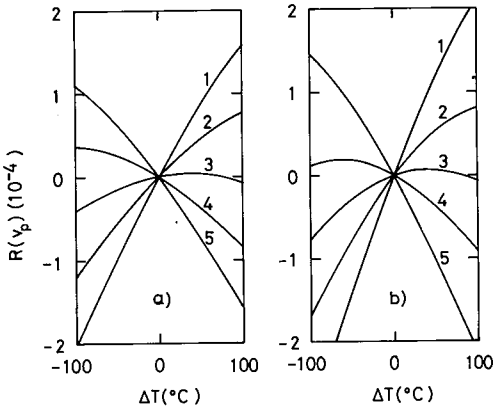

Fig.12. Relative temperature dependence of the phase velocity $R(v_p)$. The layered structure is; (a) ZnO-SiO_2 with $kd_1 = 2.8$ (curve 1), 2.85 (2), 2.9 (3), 2.95 (4) and 3.0 (5); (b) ZnO-SiO_2-$Si_{(011)<100>}$ with $kd_1 = 0.2$, and $kd_2 = 0.6$ (1), 0.57 (2), 0.55 (3), 0.53 (4) and 0.5 (5).

Using values of $TC(e)$ and $TC(\epsilon^S)$ for ZnO measured by Tokarev et al. [17], it has been found from numerical calculations that the effect $TC_2(v_p)$ due to non-zero $TC(e)$ and $TC(\epsilon^S)$ is nearly 0.02 ppm/° C, while $TC_2(v_g) \simeq 0.15$. Therefore $TC_2(v_p)$ and $TC_2(v_g)$ are negligibly small, as expected from the fact that the relative change $\Delta v/v$ of the phase velocity due to the piezoelectric effect is, at most, 1.8%.

In connection with the effects $TC_3(v)$, $TC_4(v)$ and $TC_5(v)$, we consider thermal expansion coefficients in a layered structure, in which the thickness of the substrate is very much larger than that of the layer. If it is assumed that different media are completely clamped at the boundary and that the stress component σ_{33} in the direction normal to the surface is zero, the expansion coefficient $\overline{\beta_i}^{(j)}$ ($i = 1$, 2 and 3) of the jth layer is given by

$$\overline{\beta_i}^{(j)} = \beta_i^{(s)} \quad \text{for } i = 1 \text{ and } 2,$$
$$\overline{\beta_3}^{(j)} = \beta_3^{(j)} + [2C_{13}^{(j)}/C_{33}^{(j)}]\,[\beta_1^{(j)} - \beta_1^{(s)}], \tag{2}$$

where $\beta_i^{(j)}$ and $\beta_i^{(s)}$ are the thermal expansion coefficients of the medium forming the jth layer and the substrate, respectively, in the x_i direction. The temperature coefficients of the layer thickness $\mathrm{TC}(d_j)$ and density $\mathrm{TC}(\overline{\rho_j})$ then become

$$\mathrm{TC}(d_j) \equiv \mathrm{d}(\ln d_j)/\mathrm{d}T = \overline{\beta_3}^{(j)} \tag{3}$$

$$\mathrm{TC}(\overline{\rho_j}) \equiv \mathrm{d}(\ln \overline{\rho_j})/\mathrm{d}T = -2\overline{\beta_1}^{(j)} - \overline{\beta_3}^{(j)} \tag{4}$$

Table 2 gives results of $\overline{\beta_i}$ and $\mathrm{TC}(\overline{\rho})$ for the ZnO-SiO_2-Si structure. Similarly, the internal stress induced by the difference of thermal expansion coefficients is given by

$$\mathrm{d}\sigma_{11}^{(j)}/\mathrm{d}T = -\,[C_{11}^{(j)} + C_{12}^{(j)} - 2(C_{13}^{(j)})^2/C_{33}^{(j)}] \times [\beta_1^{(j)} - \beta_1^{(s)}] \tag{5}$$

TABLE 2

Thermal expansion coefficient $\overline{\beta}$ (ppm/° C) in the layered structure

layer	ZnO			SiO_2		Si
substrate	ZnO	SiO_2	Si	SiO_2	Si	Si
$\overline{\beta_1}$	4.0	0.55	2.6	0.55	2.6	2.6
$\overline{\beta_3}$	2.1	5.5	3.5	0.55	0.3	2.6
$\mathrm{TC}(\overline{\rho})$	−10.1	−6.6	−8.7	−1.65	−4.9	−7.8

Using these results, the effects $\mathrm{TC}_3(v)$, $\mathrm{TC}_4(v)$ and $\mathrm{TC}_5(v)$ are estimated as follows. $\mathrm{TC}_3(v)$ due to the thermal expansion for d_j in the jth layer is given by

$$\mathrm{TC}_3(v) = \Sigma_j\,[\partial\,(\ln v)/\partial\,(\ln kd_j)]\,\overline{\beta_3}^{(j)} \tag{6}$$

It has been found from numerical calculations of the thickness dependence of v_p and v_g that

$$-0.12 \lesssim \partial\,(\ln v_p)/\partial\,(\ln kd_1) \gtrsim 0.01$$
$$-0.16 \lesssim \partial\,(\ln v_g)/\partial\,(\ln kd_1) \lesssim 0.08$$

for the ZnO-SiO_2 structure and that

$$-0.26 \lesssim \partial\,(\ln v_p)/\partial\,(\ln kd_1) \lesssim 0$$
$$-0.24 \lesssim \partial\,(\ln v_p)/\partial\,(\ln kd_2) \lesssim 0$$
$$-0.38 \lesssim \partial\,(\ln v_g)/\partial\,(\ln kd_1) \lesssim 0.18$$
$$-0.46 \lesssim \partial\,(\ln v_g)/\partial\,(\ln kd_2) \lesssim 0.21$$

for $ZnO\text{-}SiO_2$ -Si. Using these results and $\overline{\beta_3}$ in Table 2, it is found that TC_3 $(v_p) \cong -0.7$ to 0.1 and -0.9 to 0.1 ppm/°C for the $ZnO\text{-}SiO_2$ and $ZnO\text{-}SiO_2$-Si structure, respectively, while $TC_3(v_g) \cong -0.9$ to 0.4 and -1.4 to 0.8 for the same layered structure.

The effect $TC_4(v)$ due to the change of $TC(\rho_j)$ in the jth layer becomes

$$TC_4(v) = \Sigma_j \left[\partial (\ln v)/\partial (\ln \rho_j)\right] \left[TC(\overline{\rho_j}) - TC(\rho_j)\right] \tag{7}$$

As mentioned in section 3.1, equations for determining v_p include ρ_j only in the form $\rho_j v_p^2$. When the thickness of the jth layer is sufficiently thin compared with the wave length of SAW, ρ_j has little influence on v_p. When sufficiently thick, v_p is proportional to $\rho_j^{-0.5}$. Then,

$$-0.5 \lesssim \partial (\ln v)/\partial (\ln \rho_j) \lesssim 0$$

for both v_p and v_g. Therefore, $TC_4(v_p)$ and $TC_4(v_g)$ become -1.8 to 0 ppm/°C for $ZnO\text{-}SiO_2$, while they become -0.7 to 1.6 for $ZnO\text{-}SiO_2$ -Si.

By considering eqn. (1) and the similar equation for v_g, the effect $TC_5(v)$ due to the internal stress is given by

$$TC_5(v) \cong \Sigma_j \, 1/(2\rho_j v^2)\,(d\,\sigma_{11}^{(j)}/dT) \tag{8}$$

Substituting eqn. (5) into eqn. (8) and using values in Tables 1 and 2, TC_5 (v_p) becomes -9.3 to -5.9 and -3.8 to 3.5 ppm/°C for the layered structure with the SiO_2 and Si substrate, respectively, while $TC_5(v_g)$ becomes -10.6 to -5.9 and -4.9 to 4.8.

In view of these results, the temperature coefficients of velocities $TC(v_p)$ and $TC(v_g)$ are mainly determined by those of elastic constants $TC(C^E)$. Among five minor effects mentioned in this section, the effect of the internal stress is the greatest.

Values of $TC(C^E)$ used in this paper were estimated by assuming that $TC(C_{33}{}^E) = TC(C_{33}{}^D)$ and $TC(S_{13}{}^E) = TC(S_{12}{}^E)$, because some of them remain, as yet, undetermined. The former equality is reasonable in view of a weak piezoelectric coupling of the ZnO crystal, but the justification for assuming the latter equality is not clear. In consideration of these facts and the above-mentioned assumptions, it is concluded that $TC_a(v_p)$ and $TC_a(v_g)$ shown in Figs.6 and 7, do not have a quantitative meaning, but indicate a qualitative meaning. They indicate a qualitative feature of the linear temperature coefficients of v_p and v_g as the layer thickness changes, e.g. that the zero-temperature coefficient is realized by setting appropriate thicknesses of the ZnO and SiO_2 layers; $kd_1 \lesssim 2.9$ and $kd_2 \gtrsim 0.3$ for v_p; $kd_1 \lesssim 2.0$ and $kd_2 \gtrsim 0.1$ for v_g.

3.3 Coupling factor $\Delta v/v$

Numerical calculations for the coupling factor $\Delta v/v$ have been carried out so far by using piezoelectric constants e listed in Table 1. Typical and recent values of e and the resulting $\Delta v/v$ for the ZnO substrate are given in Table 3. Definite values of e have not yet been obtained. On the other hand, a measured value of $\Delta v/v$ is 0.447% for the c-cut ZnO crystal [22]. In order to estimate

TABLE 3

Piezoelectric constant e (C/m^2), phase velocity v_p (km/s) and coupling factor $\Delta v/v$ (%) for the ZnO crystal

e_{31}	e_{33}	e_{15}	v_p	$\Delta v/v$	Ref.
−0.61	1.14	−0.59	2.716[b]	0.708[b]	[13]
−0.62	0.96	−0.37	2.659[b]	0.351[b]	[17]
−0.35[a]	1.56[a]	−0.35[a]	2.655[b]	0.246[b]	[23]

[a] These values are transferred from d constants by using C^E listed in Table 1.

[b] Numerical calculations are carried out by using ρ, C^E and ϵ^S listed in Table 1.

values of e from the experimental values of $\Delta v/v$, the effects of e_{ij} on $\Delta v/v$ were calculated and shown in Fig.13. It is found that the effect of e_{15} is much greater than that of e_{31} and e_{33}, and that e_{33} has little influence on $\Delta v/v$. It is expected from curve 1 in Fig.13 that $e_{15} = -0.44$ C/m^2 provided that values of e_{31} and e_{33} listed in Table 1 are correct. Kino and Wagers [2] emphasized that e_{31} has an important effect on the first peak of $\Delta v/v$ and that e_{33} and e_{15} have a major effect on the second peak for the ZnO layer on the fused-quartz substrate. Under the present condition that definite values of e_{ij} have not been determined, the thickness dependence of $\Delta v/v$ in the preceding section has only a qualitative meaning. Moreover, one should consider the difference between piezoelectric constants in films and crystals, when layers are prepared by using thin film technology such as sputtering deposition.

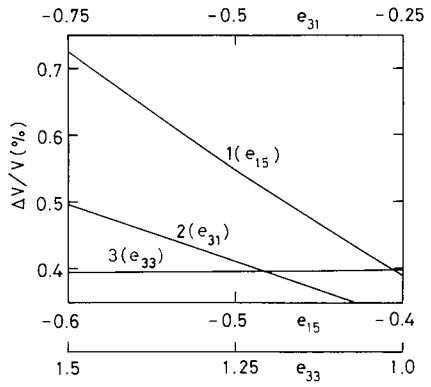

Fig.13. Effect of piezoelectric constants e_{ij} (C/m^2) on $\Delta v/v$ for the c-cut ZnO crystal; e_{15} (curve 1) at $e_{31} = -0.61$ and $e_{33} = 1.14$, e_{31}(2) at $e_{33} = 1.14$ and $e_{15} = -0.438$, and e_{33} (3) at $e_{31} = -0.61$ and $e_{15} = -0.438$.

Material constants of the SiO_2 layer have been taken as those of fused-quartz so far. It is desired that constants of the SiO_2 film, which is fabricated by integrated circuit technology such as chemical vapor deposition and thermal

oxidization of Si, are measured and used to analyze SAW properties for the combined devices.

The effects of the conductivity of Si substrates are important in practical devices. For example, Fig.8 indicates that as the conductivity σ of Si substrates increases from zero to infinity in the transducer structures (A), (B) and (C) of Fig.1, the coupling factor $\Delta v/v$ decreases, that is, the conversion loss increases. Another important effect of the conductivity of Si substrates is the interaction of SAW with free carriers of Si, which substantially affects the propagation loss of SAW [7].

4. Conclusions

Completely quantitative discussions such as the determination of the layer thickness, providing the zero-temperature coefficient and the highest electromechanical coupling, could not be carried out, because definite values of material constants for the ZnO and SiO_2 layers have not been obtained completely. The following qualitative results, however, were obtained for SAW properties of the ZnO-SiO_2-Si layered structure:

(1) The layered structure has a linear temperature coefficient of phase velocity ranging approximately from −30 to +80 ppm/° C and that of the group velocity from −50 to +130 ppm/° C.

(2) The zero-temperature coefficient of the velocities is realized by setting an appropriate thickness d_1 (ZnO layer) and d_2 (SiO_2); for the phase velocity $kd_1 \lesssim 2.9$ and $kd_2 \gtrsim 0.3$; for the group velocity $kd_1 \lesssim 2.0$ and $kd_2 \gtrsim 0.1$.

(3) One should consider the thermal expansion of the layer thickness, the change of the temperature coefficient of density and the introduction of internal stress caused by the difference of thermal expansion coefficients in the layer and the substrate as well as the temperature coefficients of elastic constants in order to determine the temperature coefficients of the phase and group velocities with an accuracy of a few ppm/° C.

(4) The coupling factor for the ZnO-SiO_2-Si structure has the first peak near $kd_1 \simeq 0.2$ and the second peak near $kd_1 \simeq 2.8$ regardless of the SiO_2 layer thickness and the crystallographic and electric properties of the Si substrate.

(5) The maximum value of the first peak is obtained for the layered structure with the (001) cut <100> and <110> propagating Si substrate.

(6) The value of the coupling factor near the second peak attains a value about 2.5 times larger than that for the ZnO crystal.

Accordingly, it is possible to make SAW devices having the high electromechanical coupling and the temperature-stability for center frequency and delay time, to which integrated circuit devices are normally associated, by using the ZnO-SiO_2-Si layered structure.

References

1 P.H. Carr, New temperature compensated materials for SAW devices, IEEE Ultrason. Symp., Milwaukee, 1974, pp. 286.

2 G.S. Kino and R.S. Wagers, Theory of interdigital couplers on nonpiezoelectric substrates, J. Appl. Phys., 44 (1973) 1480.
3 F.S. Hickernell, The acoustic properties of oxide films and their application to acoustic surface wave devices, J. Solid State Chem., 12 (1975) 225.
4 T.E. Parker and M.B. Schultz, SiO_2 film overlays for temperature-stable surface acoustic wave devices, Appl. Phys. Lett., 26 (1975) 75.
5 K.L. Davis, Surface acoustic waves with nearly dispersion-free propagation in a layered silicon configuration, J. Appl. Phys., 45 (1974) 3255.
6 A. Venema and J.J.M. Dekkers, Enhancement of surface-acoustic-wave piezoelectric coupling in three-layer substrates, IEEE Trans. Microwave Theory and Tech., MTT-23 (1975) 765.
7 B.T. Khuri-Yakub and G.S. Kino, A monolithic zinc-oxide-on-silicon convolver, Appl. Phys. Lett., 25 (1974) 188.
8 L.A. Coldren, Effect of bias field in a zinc-oxide-on-silicon acoustic convolver, Appl. Phys. Lett., 25 (1974) 473.
9 K. Ohji, T. Tohda, K. Wasa and S. Hayakawa, Highly oriented ZnO films by rf sputtering of hemispherical electrode system, J. Appl. Phys., 47 (1976) 1726.
10 K.A. Ingebrigsten and A. Tonning, Excitation of elastic waves in crystals, IEEE Trans. Microwave Theory and Tech., MTT-17 (1969) 827.
11 O.L. Anderson, Determination and some uses of isotropic elastic constants of polycrystalline aggregates using single-crystal data. In W.P. Mason (Ed.), Physical Acoustics, Vol. III B, Academic Press, New York, 1965.
12 H.J. McSkimin, Measurement of ultrasonic wave velocities and elastic moduli for small solid specimens at high temperatures, J. Acoust. Soc. Am., 31 (1959) 287.
13 H. Jaffe and D.A. Berlincout, Piezoelectric transducer materials, Proc. IEEE, 53 (1965) 1372.
14 D.G. Fink, Electronics Engineers' handbook, McGraw-Hill, New York, 1975.
15 H.B. Huntington, The elastic constants of crystals. In F. Seitz and D. Turnbull (Eds.), Solid State Physics, Vol. 7, Academic Press, New York, 1958.
16 D.A. Berlincout, H. Jaffe and L.R. Shiozawa, Electro-elastic properties for the sulfides, selenides, and tellurides of zinc and cadmium, Phys. Rev., 129 (1963) 1009.
17 E.F. Tokarev, I.B. Kobyakov, I.P. Kuzmina, A.N. Lobachev and G.S. Pado, Elastic, dielectric, and piezoelectric properties of zincite in the 4.2—800° K temperature range, Sov. Phys.-Solid State, 17 (1975) 629.
18 G.W. Farnell, Properties of elastic surface waves. In W.P. Mason and R.N. Thurston (Eds.), Physical Acoustics, Vol. VI, Academic Press, New York, 1970.
19 J.J. Cambell and W.R. Jones, A method for estimating optimal crystal cuts and propagation directions for excitation of piezoelectric surface waves, IEEE Trans. Sonics and Ultrason., SU-15 (1972) 209.
20 A.L. Nalamwar and M. Epstein, Effects of applied strain in ZnO thin-film SAW devices, IEEE Trans. Sonics and Ultrason., SU-23 (1976) 144.
21 K.L. Chopra, Thin Film Phenomena, McGraw-Hill, New York, 1969, Chap. V.
22 H.B. Schultz and J.H. Matsinger, Rayleigh-wave electromechanical coupling constants, Appl. Phys. Lett., 20 (1972) 367.
23 D.F. Crisler, J.J. Cupal and A.R. Moore, Dielectric, piezoelectric, and electromechanical coupling constants of zinc oxide crystals, Proc. IEEE, 56 (1968) 225.